Unipolar space-charge limited current through layers with a disparate concentration of shallow traps: Experiment and model

Arne Fleissner,[a] Wieland Weise, and Heinz von Seggern
Electronic Materials Department, Institute of Materials Science, Darmstadt University of Technology, Petersenstrasse 23, D-64287 Darmstadt, Germany

(Received 1 September 2004; accepted 5 November 2004; published online 20 January 2005)

The influence of the spatial distribution of trap states on unipolar space-charge limited current (SCLC) is investigated experimentally and theoretically. Thin-layered films of the small molecule organic semiconductor N,N′-di(1-naphtyl)-N,N′-diphenylbenzidine (α-NPD) are vapor deposited on indium tin oxide, with aluminum as the counter electrode. The small molecule 4,4′,4″-tris-[N-(1-naphtyl)-N-(phenylamino)]-triphenylamine (1-NaphDATA), which creates well-known shallow traps for holes, is used as dopant. The realized organic films consist of three layers, one of which is homogeneously doped. The influence of the spatial position of the doped layer on the current–voltage characteristics of the diodes is examined. Compared to an undoped device, the current density is strongly decreased and varies over orders of magnitude for the different spatial positions of the doped layer. It is shown that traps near the injecting electrode have the most pronounced effect on SCLC. A model for unipolar SCLC through a system of homogeneous layers with different trapping parameters for shallow traps is presented. The model quantitatively describes the experimental data and is used to calculate the spatial distributions of the charge-carrier density and the electric-field strength in the differently doped devices. [DOI: 10.1063/1.1840094]

I. INTRODUCTION

Space-charge limited current (SCLC) occurs in insulators or semiconductors when injected excess charge carriers, which build up a space charge screening the external electric field, dominate the electric current. Electronic states present in the energy gap of the material will affect the SCLC. The influence of different densities and energy distributions of such trap states on SCLC characteristics have been thoroughly examined theoretically and experimentally.[1–3] However, the common approach that is applied to interpret experimental results assumes a homogeneous spatial distribution of traps.

A number of publications has also dealt with inhomogeneous spatial distributions.[4–8] However, among the majority of theoretical analyses, only few works correlate experimental data with a theoretical framework.[9,10] There may exist two main reasons: On the one hand it is complicated to extract the spatial distribution of trap states in a certain device from SCLC analysis,[11] on the other hand it seems difficult to fabricate a device with a specified spatial trap distribution in order to study its effect on SCLC characteristics.

In the present paper the latter task is performed by vapor deposition of thin-layered films of a small molecule organic semiconductor. In this approach a second small molecule can be used as dopant in order to deliberately introduce well-known shallow trap states. The realized organic films consist of three layers, one of which is homogeneously doped. The influence of the spatial position of the doped layer on the current–voltage (J–V) characteristics is examined.

In order to analytically describe the experimental results, a model for unipolar SCLC through a system of homogeneous layers with different trapping parameters for shallow traps is presented. The model quantitatively describes the experimental data. It is also used to calculate the spatial distributions of the charge-carrier density and the electric-field strength in the differently doped devices.

II. EXPERIMENT

The schematic cross section of the processed devices is presented in Fig. 1. The diodes consist of the organic semiconductor sandwiched between indium tin oxide (ITO) and aluminum electrodes. The organic film had an overall thickness of 210 nm for all samples. The hole transport material

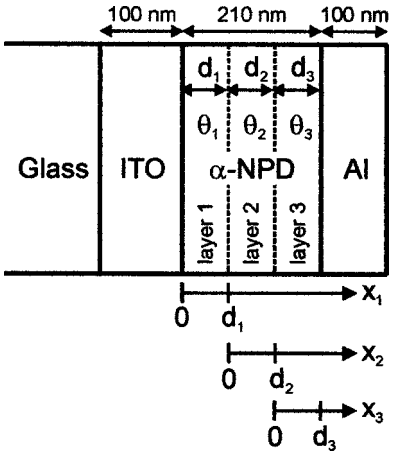

FIG. 1. Schematic of the investigated devices. The variables relate to the theoretical model. θ_i is the trapping parameter, x_i the spatial coordinate, and d_i the thickness of the respective layer.

[a]Electronic mail: fleissner@e-mat.tu-darmstadt.de

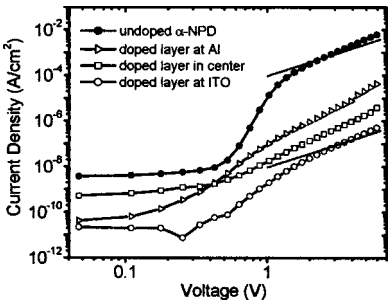

FIG. 2. Current–voltage characteristics of the undoped and the three differently doped devices in double-logarithmic scale. The two straight lines with a slope of two are guides to the eye. The SCLC behavior is observed for voltages above approximately 1.5 V. The voltage given here is the external applied voltage corrected by the built-in potential of −0.6 V.

N,N′-di(1-naphtyl)-N,N′-diphenylbenzidine (α-NPD) was used as the matrix material. The energy levels for the highest occupied molecular orbital (HOMO) and the lowest unoccupied molecular orbital (LUMO) are 5.4 and 2.3 eV, respectively.[12] 4,4′,4″-tris-[N-(1-naphtyl)-N-(phenylamino)]-triphenylamine (1-NaphDATA) was used as the doping material. It is known to create hole traps in α-NPD with an energetic depth of approximately 0.5 eV.[13] Three devices were processed, in which a 70-nm layer was doped with 1-NaphDATA. The doped layer was either located directly at the ITO electrode (layer 1), in the middle of the α-NPD film (layer 2), or directly at the aluminum electrode (layer 3). Furthermore, a device with an undoped α-NPD film of 210-nm thickness was prepared.

The devices were processed by vacuum sublimation of the organic molecules on an ITO-coated glass substrate (Merck). The 100-nm-thick ITO, serving as the transparent anode, had previously been structured in a photolithographic process. The substrates were cleaned in a detergent solution, rinsed with distilled water, dried in N_2, and finally kept in an UV-generated ozone atmosphere for 15 min. The organic molecules were deposited in a vacuum chamber at a pressure of 10^{-6} mbar. The deposition rate of the matrix material α-NPD was 10 Å/s. Doping with 3 vol% 1-NaphDATA in the respective layers was achieved by codeposition of the dopant material at a rate of 0.3 Å/s. Finally, 100-nm aluminum was deposited by thermal evaporation at a rate of 5 Å/s to form the cathode. The resulting diodes have an active area of 10 mm^2. For measurements the samples were transferred to a nitrogen atmosphere glove box without exposure to ambient air.

The $J-V$ characteristics were measured at room temperature with a Hewlett–Packard parameter analyzer (HP 4155A). Simultaneously, possible luminescence was detected by means of photodiodes.

III. EXPERIMENTAL RESULTS

Figure 2 displays the measured current–voltage characteristics of the devices in double-logarithmic scale. The shown voltage values are the externally applied voltages corrected by the built-in potential of −0.6 V. The built-in potential is assumed as the difference of the work functions of the electrode materials [4.8 eV for ozone-treated ITO (Ref. 14) and 4.2 eV for aluminum]. All $J-V$ characteristics enter the SCLC regime and show approximately the same slope for voltages above 1.5 V. Basic SCLC theory[1,2] predicts a slope of two in the double-logarithmic $J-V$ characteristics, whereas a linear fit on the experimental data between 2 and 4 V yields slopes between 2.8 and 3.1. This discrepancy might be explained by uncertainties in the value of the built-in potential. The slopes of the $J-V$ characteristics in the SCLC regime vary substantially when the assumed value for the built-in potential is changed by some tens of a volt. Slopes of approximately two occur in the SCLC regime of the measured $J-V$ characteristics for an assumed built-in potential of −1.4 V. This value is high compared to the given difference of the work functions of the electrode materials, but might be explained by interface dipoles. However, the actual value of the built-in potential is of no importance to the following considerations and calculations, since only the current densities of the different devices will be compared with each other.

In the SCLC regime the doped devices show a current density that is orders of magnitude smaller compared to the undoped device. The regime at voltages below 1 V is presumably controlled by charge carriers introduced by residual impurities in the material. Its interpretation is not the scope of this paper.

The barrier of 1.9 eV for electron injection from aluminum into the LUMO of α-NPD is high compared to the barrier of 0.6 eV for hole injection from ITO into the HOMO. Furthermore, α-NPD is a hole transport material. For these reasons, the current may be considered to be a unipolar hole current. This assumption is supported by the absence of any electroluminescence for all examined voltages.

The spatial position of the doped layer, i.e., the layer with high trap density, has a significant effect on the $J-V$ characteristics, as shown in Fig. 2. This effect is substantial: For a voltage of 6 V the current density of the device with the doped layer adjacent to the hole injecting ITO electrode is approximately two orders of magnitude smaller than for the device with the doped layer at the hole collecting aluminum electrode. The current density of the device with the doped layer in the middle of the organic film lies in between the other two $J-V$ characteristics. It seems intuitive that traps located at the injecting electrode lead to a stronger reduction of the current density than those located at the counter electrode, if one keeps in mind that in the case of SCLC the vast majority of injected charge carriers is located near the injecting electrode.[1,2]

IV. MODEL

For SCLC in diodes of various geometries with a uniform distribution of shallow traps either in the vicinity of the emitting or the counter electrode, respectively, a theoretical study was presented by Nicolet.[4] However, to reproduce the experimental situation, a model is necessary that comprises at least three layers with different trapping parameters. Therefore, a general expression for SCLC in a system of planar geometry with n layers with different trapping param-

eters is derived here. This derivation is presented in some detail, since it yields analytical expressions for the charge-carrier density and the electric-field strength in dependence on the spatial coordinate. These equations will be employed to reveal the different spatial distributions of those quantities in the different devices.

The analytical treatment is based on the following assumptions:

(a) unipolar SCLC,
(b) currents due to diffusion and thermally generated charge carriers can be neglected, and
(c) the traps are shallow, only the trap-controlled SCLC regime is accounted for, i.e., only voltages above the ohmic/SCLC transport crossover and below the trap-filled limit are considered.

In the trap-controlled SCLC the trapping parameter θ is used to describe the ratio between the free charge-carrier density $n_f(x)$ and the total charge-carrier density $n(x)$,

$$\theta = \frac{n_f(x)}{n_f(x)+n_t(x)} = \frac{n_f(x)}{n(x)} \quad \text{or} \quad n_f(x) = \theta n(x), \tag{1}$$

where $n_t(x)$ denotes the trapped charge-carrier density.

In the case of shallow traps considered here, the (quasi) Fermi level for the holes is energetically at least $2kT$ below the trap states so that their occupation can be described by Boltzmann statistics. The trapping parameter θ then is only controlled by the energetic distribution and density of traps, which are assumed to be homogeneously distributed within each single layer.

The dependence of space-charge limited current on voltage and on the material parameters is derived from the expression for the drift current density j

$$j = q\mu n_f(x)F(x) = q\mu\theta n(x)F(x) \tag{2}$$

and from Poisson's law

$$\frac{\partial F(x)}{\partial x} = \frac{q}{\varepsilon\varepsilon_0}n(x), \tag{3}$$

where Eq. (1) has been introduced into Eq. (2). q is the charge of the charge carriers, μ the charge-carrier mobility, ε the relative permittivity of the material, and F the electric-field strength. While μ and ε are considered to be identical for all layers, each layer i may have an individual thickness d_i and trapping parameter θ_i. The origin of the spatial coordinate x_i is at the beginning of each layer i, as can be seen in Fig. 1.

With the boundary-condition $F_i^0 = F_i(x_i=0)$, substitution of Eq. (2) in Eq. (3) and integration yields

$$F_i(x_i) = \sqrt{\frac{2\,jx_i}{\theta_i\varepsilon\varepsilon_0\mu} + (F_i^0)^2}. \tag{4}$$

The charge carriers are injected into layer 1 from the electrode at $x_1=0$. As in common SCLC theory, this contact is assumed to be ohmic and therefore the charge-carrier density at $x_1=0$ is infinite. In order to ensure a finite value for the current, this leads to the boundary-condition $F_1^0=0$. For layers $i>1$, however, charge carriers are injected from the backplane of the respective previous layer, where the charge-carrier density has a finite value. The boundary conditions for those layers are obtained from the continuity of the electric field, i.e., by matching the electric-field strength at the interface between two layers: $F_i^0 = F_{i-1}(x_{i-1}=d_{i-1})$.

Integration of Eq. (4) over the entire layer thickness d_i yields the voltage drop over one single layer

$$V_i(d_i,j) = -\frac{\theta_i\varepsilon\mu}{3j}\left\{\left[\frac{2\,jd_i}{\theta_i\varepsilon\varepsilon_0\mu} + (F_i^0)^2\right]^{3/2} - (F_i^0)^3\right\}. \tag{5}$$

The total voltage drop over the entire system of layers is the sum of the voltage drops over the individual layers. The current density is the same in all layers due to the continuity of the electric current. Therefore, summation over all V_i, introducing the respective boundary conditions for F_i^0, and solving for j finally yields the $j-V$ dependence for the entire system

$$j = \frac{9}{8}\varepsilon\varepsilon_0\mu\frac{V^2}{\alpha}$$

$$\text{with } \alpha = \left\{\sum_{i=1}^{n}\theta_i\left[\left(\sum_{k=1}^{l}\frac{d_k}{\theta_k}\right)^{3/2} - \left(\sum_{l=1}^{i-1}\frac{d_i}{\theta_l}\right)^{3/2}\right]\right\}^2. \tag{6}$$

To check the validity of Eq. (6) two limiting cases are considered. Setting $\theta_i=\theta$ corresponds to a homogeneous system with the trapping parameter θ and thickness $d=\Sigma d_i$. Under these conditions, Eq. (6) reduces to the well-known formula for trap-controlled SCLC $j=(9/8)\varepsilon\mu\theta U^2/d^3$. With $n=1$ and $\theta_1=\theta$ Eq. (6) should describe trap-controlled SCLC through a system with just the thickness d_1. Indeed it yields $j=(9/8)\varepsilon\mu\theta U^2/d_1^3$ in this case.

In the paper of Sworakowski[5] a spatially dependent trap distribution function was introduced. The result given by Eq. (6) may also be derived from this approach by defining appropriate step functions for the spatial trap distribution. By solving the expression given by Sworakowski, including double integration of the distribution function, Eq. (6) is confirmed.

In the conducted experiment the number of layers $n=3$ and $d_1=d_2=d_3$. Therefore, with the total thickness $d=3d_1$, Eq. (6) can be written as

$$j = j_0\Phi \quad \text{with} \quad j_0 = \frac{9}{8}\varepsilon\varepsilon_0\mu\frac{V^2}{d^3}$$

$$\text{and} \quad \Phi = 27\left[\theta_1\left(\frac{1}{\theta_1}\right)^{3/2} + \theta_2\left(\frac{1}{\theta_2}+\frac{1}{\theta_1}\right)^{3/2} - \theta_2\left(\frac{1}{\theta_1}\right)^{3/2} + \theta_3\left(\frac{1}{\theta_3}+\frac{1}{\theta_2}+\frac{1}{\theta_1}\right)^{3/2} - \theta_3\left(\frac{1}{\theta_2}+\frac{1}{\theta_1}\right)^{3/2}\right]^{-2}. \tag{7}$$

Here, j_0 corresponds to SCLC through an undoped system with thickness d, and Φ, depending only on the θ_i, is the factor by which j_0 is reduced when traps are introduced into the system. The doping of one specific layer can be modeled by setting the respective $\theta_i=\theta$ and the other two $\theta_i=1$. Setting θ_i to unity means that all injected charge carriers are free

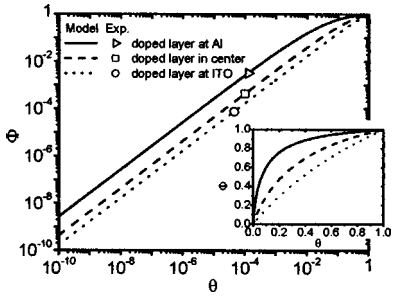

FIG. 3. Plots of Φ vs θ in double-logarithmic scale as given by Eqs. (8)–(10). The open symbols mark the respective values for Φ that were obtained experimentally from the three doped devices. It can be seen that the model within some tolerance correlates the experimentally determined Φ with the same value for θ. The inset shows the plots of Φ vs θ in linear scale.

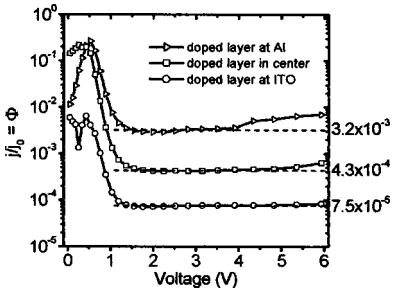

FIG. 4. Ratio of the current values j of the differently doped devices to the current values j_0 of the undoped device. In the trap-controlled SCLC regime, i.e., for voltages above approximately 1.5 V, j/j_0 settles to a certain level, thus yielding the factor Φ, by which the current is reduced by introducing the doped layer.

charge carriers as in the undoped material.[15] The trapping parameter θ is the same for all doped devices, irrespective of the position of the doped layer, because the energetic distribution and density of the traps are independent of the location of the doped layer. For the three different cases the expressions Φ_{ITO}, Φ_{center}, and Φ_{Al} are obtained as functions of θ, whereby the subscript denotes the position of the doped layer.

$$\Phi_{\mathrm{ITO}} = \left[\left(\frac{1}{27\theta} \right)^{1/2} - \left(\frac{1}{3\theta} \right)^{3/2} + \left(\frac{1}{3\theta} + \frac{2}{3} \right)^{3/2} \right]^{-2}, \tag{8}$$

$$\Phi_{\mathrm{center}} = \left[\left(\frac{1}{3} \right)^{3/2} + \theta \left(\frac{1}{3\theta} + \frac{1}{3} \right)^{3/2} - \theta \left(\frac{1}{3} \right)^{3/2} + \left(\frac{1}{3\theta} + \frac{2}{3} \right)^{3/2} - \left(\frac{1}{3\theta} + \frac{1}{3} \right)^{3/2} \right]^{-2}, \tag{9}$$

$$\Phi_{\mathrm{Al}} = \left[\left(\frac{2}{3} \right)^{3/2} + \theta \left(\frac{1}{3\theta} + \frac{2}{3} \right)^{3/2} - \theta \left(\frac{2}{3} \right)^{3/2} \right]^{-2}. \tag{10}$$

Equations (8) and (10) conform to the results derived by Nicolet[4] for shallow traps in the vicinity of the emitting electrode or the counter electrode, respectively.

Introducing Eq. (7) to Eqs. (4) and (2) leads to expressions for the electric-field strength and the charge-carrier density in dependence on the spatial coordinate x_i and the voltage V.

$$F_i(x_i) = \sqrt{\frac{9 x_i V^2 \Phi}{4 \theta_i d^3} + (F_i^0)^2}, \tag{11}$$

$$n_i(x_i) = \frac{9 V^2 \Phi \varepsilon \varepsilon_0}{8 d^3 q \theta_i F_i(x_i)}. \tag{12}$$

V. RESULTS AND DISCUSSION

Figure 3 shows the plots of Φ vs θ. The closer the doped layer is located to the injecting ITO electrode, the smaller is the factor Φ. This is in accordance with the experimental results shown in Fig. 2. The plots converge to unity for $\theta = 1$, since the influence of traps vanishes.

A quantitative comparison between the theoretical and experimental results can be achieved by calculating Φ from the experimental $J-V$ characteristics, i.e., the factor by which the current is decreased relatively to the undoped device. For this the current values j of the $J-V$ characteristics of the doped systems are normalized to the current values j_0 of the undoped system. The resulting plots of j/j_0 vs V are depicted in Fig. 4. For voltages above approximately 1.5 V, which is the voltage regime in which SCLC is actually observed (see Fig. 2), the J/j_0 plots indeed settle to a certain level that yields the respective experimentally obtained Φ. Averaging the data between 2 and 4 V yields $\Phi_{\mathrm{ITO}} = 7.5 \times 10^{-5}$, $\Phi_{\mathrm{center}} = 4.3 \times 10^{-4}$, and $\Phi_{\mathrm{Al}} = 3.2 \times 10^{-3}$.

These values for Φ are marked in the corresponding theoretically obtained plots of Φ vs θ shown in Fig. 3. Since the basis of the model was the assumption that θ is only dependent on the energetic distribution and density of traps, it should have the same value for all three systems, regardless of where the doped layer is located in the device. In Fig. 3 it can be seen that the experimentally obtained Φ values indeed are expressed by the analytic equations using similar values for θ in all three cases. With Eqs. (8)–(10), the respective θ values are calculated to be $\theta_{\mathrm{ITO}} = 0.5 \times 10^{-4}$, $\theta_{\mathrm{center}} = 1.0 \times 10^{-4}$, and $\theta_{\mathrm{Al}} = 1.3 \times 10^{-4}$, differing by a factor of 2.6. These values average to 0.9×10^{-4}. This is also in good agreement with a value for θ obtained from a device that was prepared in the same way as described above, but which was doped homogeneously over the entire film thickness (results not shown here). In this case $\Phi = \theta$ and a value of 10^{-4} was obtained.

It is instructive to calculate the spatial distribution of the total charge-carrier density and the electric-field strength for the three differently doped devices from the theoretical model. These can be obtained from Eqs. (12) and (11), utilizing the respective Φ given by Eqs. (8)–(10).

In the case of SCLC through a homogeneous film, the majority of charge carriers is located at the injecting electrode and their density decreases with $x^{-1/2}$. In contrast, Fig. 5(a) shows that in all three devices the majority of charge carriers is located in the doped layer, irrespective of its position. Within all layers the charge-carrier density decreases again with $x^{-1/2}$. Due to the small trapping parameter of $\theta = 10^{-4}$, effectively only the trapped charge carriers contribute to the total charge-carrier density in the doped layers. Thus, even though only one third of each device is doped, the vast majority of injected charge carriers resides in the traps.

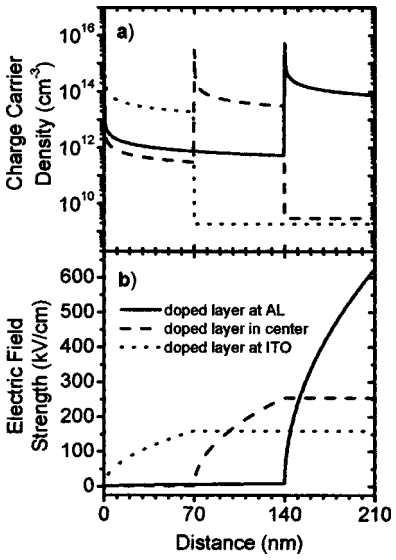

FIG. 5. Spatial distributions of (a) the charge-carrier density and (b) the electric-field strength in the three differently doped devices. The plots are calculated from Eqs. (8)–(12) of the theoretical model for a voltage of 3 V. The relative permittivity is set to $\varepsilon=3$ as typical for organic semiconductors, the charge-carrier charge to $q=+e$ for holes, and the trapping parameter in the doped layers to the experimentally determined value of $\theta=10^{-4}$.

The distribution of injected charge carriers within the devices is reflected by the spatial distribution of the electric-field strength, which changes considerably only in the respective doped layer. Figure 5(b) shows that the highest field strength occurs in the device, in which the doped layer is located adjacent to the aluminum cathode, whereas the field strength is the smallest in the device with the doped layer at the hole injecting ITO anode. This can explain the deviations of the normalized currents from a constant value at higher voltages that are observed in Fig. 4. Under the influence of an electric field, the effective depth of a trap can be reduced by the Poole–Frenkel effect (see, e.g., Kao and Hwang[2]). A reduction of the trap depth leads to an increase of the ratio between free and total charge carriers and therefore of the trapping parameter θ. Thus, also the ratio Φ between the current density of the doped and the undoped device is not constant anymore but increases at higher voltages. This effect should be most pronounced if the doped layer is adjacent to the Al electrode, since this device exhibits the highest field strength in the doped region for a given voltage. This indeed applies to the experimental data, as can be seen in Fig. 4.

From the comparison of theoretical and experimental results it can be concluded that the analytical solution proposed above for a system comprising differently doped layers is valid and capable to describe such a system in the shallow trap-controlled, unipolar SCLC regime. This could be useful for the modeling of devices in which functional doped layers are introduced into a transport film, e.g., in order to balance electron and hole transport in an organic light-emitting diode (OLED). The factor Φ, by which the current decreases, and the spatial distributions of charge-carrier density and electric-field strength can be calculated analytically for any system with homogeneously doped layers, once the trapping parameters θ of the individual layers are known. Those can be determined by examining single layer devices with the respective parameters.

Furthermore, the application of the presented model is not necessarily limited to systems comprising layers with different trap densities. θ was defined in Eq. (1) as the ratio between trapped and total injected charge-carrier density. In this approach, trapped charge carriers do not take part in the transport, while free charge carriers do so with the mobility μ. One could also assume all injected charge carriers to take part in the transport but with a reduced mobility $\theta\mu$. In this case θ is dependent on the average time the charge carriers reside in traps. This would again introduce θ into Eq. (2) as before, not via a reduced amount of free charge carriers, but via a reduced mobility, thus leaving the mathematical description of the system and the derivation unchanged. This illustrates that the model can be used for any system of layers with different mobility. Different mobilities do not necessarily have to be due to doping but, for example, can be due to different morphology, degree of order, or due to layers constituted of different materials.

VI. CONCLUSIONS

SCLC measurements on films of organic semiconductors with distinctive spatial distributions of shallow traps are presented. In the investigated devices one third of the organic film—either adjacent to the injecting electrode, in the center of the device, or adjacent to the counter electrode—exhibits a homogeneous high trap density that was realized by doping. Compared to an undoped device, the $J-V$ characteristics show a strong decrease of the current density. They vary over orders of magnitude among the three investigated devices, whereby the current density decreases stronger, the closer the doped layer is located to the injecting electrode. Traps near the injecting electrode have the most pronounced effect on charge transport in SCLC.

An analytical model for unipolar SCLC through a system of homogeneous layers with different trapping parameters for shallow traps is presented, which is also suitable for layers with different mobilities in general. The proposed model results in an analytical expression for the $J-V$ dependence of such a system. The model is able to reproduce the experimental results quantitatively.

The spatial distribution of the charge-carrier density and the electric-field strength is calculated from the model for the three differently doped devices. It is found that the majority of charge carriers resides in trap states, irrespective of the position of the doped layer within the device. The results for the electric-field strength allow one to understand the experimental data in more detail.

ACKNOWLEDGMENT

This work was supported by the Deutsche Forschungsgemeinschaft (DFG) through Sonderforschungsbereich 595.

[1]M. A. Lampert and P. Mark, *Current Injection in Solids* (Academic, New York, 1970).
[2]K. C. Kao and W. Hwang, *Electrical Transport in Solids* (Pergamon, Oxford, 1981).

[3]V. R. Nikitenko, H. Heil, and H. von Seggern, J. Appl. Phys. **94**, 2480 (2003).
[4]M. A. Nicolet, J. Appl. Phys. **37**, 4224 (1966).
[5]J. Sworakowski, J. Appl. Phys. **41**, 292 (1970).
[6]W. Hwang and K. C. Kao, Solid-State Electron. **15**, 523 (1972).
[7]J. S. Bonham, Aust. J. Chem. **31**, 2117 (1978).
[8]C. Schnittler, Phys. Status Solidi A **52**, K53 (1979).
[9]P. Delannoy, M. Schott, and J. Berrehar, Phys. Status Solidi A **32**, 577 (1975).
[10]G. W. Bak, J. Phys.: Condens. Matter **8**, 4145 (1996).
[11]J. Sworakowski and S. Nespurek, J. Appl. Phys. **65**, 1559 (1989).
[12]I. G. Hill and A. Kahn, J. Appl. Phys. **86**, 4515 (1999).
[13]N. von Malm, R. Schmechel, and H. von Seggern, Synth. Met. **126**, 87 (2002).
[14]K. Sugiyama, H. Ishii, Y. Ouchi, and K. Seki, J. Appl. Phys. **87**, 295 (2000).
[15]The undoped host material α-NPD also contains traps (see Ref. 13), which are intrinsic to the material. Therefore, not all injected charge carriers are free charge carriers. However, this situation is already reflected by the mobility μ of the host material and thus in the current–voltage dependence of the undoped device, to which the doped devices are compared to. The considered trapping parameter θ reflects only the additional traps introduced by doping.